Way, M., Gooch, J., Pope, B., & Weeds, A. G. (1989) *J. Cell Biol. 109*, 593-605.
Yamamoto, K., Sekine, T., & Kanaoka, Y. (1977) *Anal. Biochem. 79*, 83-94.
Yin, H. L., & Stossel, T. P. (1979) *Nature (London) 281*, 583-586.
Yin, H. L., Kwiatkowski, D. J., Mole, J. E., & Cole, F. S. (1984) *J. Biol. Chem. 259*, 5271-5276.

Site-Directed Mutagenesis To Probe Protein Folding: Evidence That the Formation and Aggregation of a Bovine Growth Hormone Folding Intermediate Are Dissociable Processes

S. Russ Lehrman,*,‡ Jody L. Tuls,‡ Henry A. Havel,‡,§ Royal J. Haskell,‡ Simpson D. Putnam,‡ and Che-Shen C. Tomich‖

Control Development and Molecular Biology Research, The Upjohn Company, Kalamazoo, Michigan 49001

Received June 11, 1990; Revised Manuscript Received February 27, 1991

ABSTRACT: Bovine growth hormone (bGH) forms a stable folding intermediate that aggregates at elevated concentrations (>10 μM). Thermodynamic and kinetic studies have shown that the formation of this bGH folding intermediate and its aggregation are separate processes, implying that selective modifications of bGH can lead to their independent modulation. In addition, a bGH region that includes amino acid residues 109–133 appears to be directly involved in this aggregation process. Human growth hormone (hGH), which is unable to aggregate via this mechanism, differs from the bovine primary sequence at eight positions within this protein region. We have characterized the folding of a bGH analogue that contains the hGH sequence between amino acid residues 109–133 (8H-bGH) at low and high concentrations. The equilibrium folding characteristics of bGH and 8H-bGH are similar when monitored at low protein concentrations ($\leq$2 μM). The wild-type and analogue proteins have equivalent denaturation midpoints when equilibrium unfolding is monitored by the use of far-UV circular dichroism, second-derivative UV, or fluorescence. In addition, the enhanced fluorescence that is associated with the formation of the bGH monomeric folding intermediate (Havel, H. A., et al. (1988) *Biochim. Biophys. Acta 955*, 154–163) is observed for 8H-bGH under similar conditions. In contrast, partial denaturation of 8H-bGH at higher concentrations (>2 μM) leads to significantly less aggregation than is observed for bGH. This result is obtained from near-UV CD spectroscopy, kinetic folding, size-exclusion chromatography, and dynamic light-scattering data. For example, the equilibrium constants for the formation of soluble bGH and 8H-bGH aggregates, determined from the concentration dependence of the near-UV circular dichroism signal, are 1.6×10^5 and 1.4×10^4 M^{-1}, respectively. In addition, 70 and 34% precipitation of bGH and 8H-bGH occur, respectively, by use of a two-step procedure that indirectly determines the amount of aggregation that occurs following partial denaturation. We conclude that the formation of the bGH folding intermediate and its subsequent aggregation can be independently attenuated through structural modification. Molecular characteristics of the wild-type and analogue proteins that may account for these behaviors are discussed.

Growth hormones are single-domain proteins containing 190–192 amino acid residues and two intramolecular disulfide bonds. Porcine growth hormone (pGH)[1] and bovine growth hormone (bGH) share 92% primary structural identity, and pGH has been shown to form an antiparallel four α-helix bundle (Abdel-Meguid et al., 1987). The folding of bGH has been studied in detail (Burger et al., 1966; Holladay et al., 1974; Brems et al., 1985). These studies demonstrate that the mechanism of folding for this protein proceeds via one or more intermediates. A bGH folding intermediate has been identified by use of several spectrophotometric and physicochemical techniques including near- and far-UV circular dichroism (CD), high-performance size-exclusion chromatography (HP-SEC), and dynamic light scattering (Havel et al., 1986; Brems et al., 1986). This intermediate has the characteristics of a molten globule (Brems & Havel, 1989) and is less soluble than the native and denatured forms of bGH in aqueous buffers due to its tendency to form insoluble aggregates (Brems, 1988). Although human growth hormone also associates to form higher molecular weight species (Stolar et al., 1984), this does not occur via the aggregation of a folding intermediate (Brems et al., 1990).

bGH fragments that include residues 109–133 interact with the bGH folding intermediate and inhibit bGH aggregation (Brems et al., 1986, 1987b). In addition, these protein fragments self-aggregate with concomitant α-helix formation.

* Correspondence should be addressed to this author at The Upjohn Company, Control Development 4861-259-12, 7000 Portage Road, Kalamazoo, MI 49001.
‡ Control Development.
§ Present address: Eli Lilly & Co., Indianapolis, IN 46285-0835.
‖ Molecular Biology Research.

[1] Abbreviations: BCA, bicinchoninic acid; bGH, bovine growth hormone; CD, circular dichroism spectroscopy; GdmCl, guanidinium chloride; hGH, human growth hormone; HPLC, high-pressure liquid chromatography; MRE, mean residue ellipticity; pGH, porcine growth hormone; SIMS, secondary-ion mass spectrometry.

0006-2960/91/0430-5777$02.50/0

Table I: GdmCl Denaturation Midpoints of bGH, 8H-bGH, and hGH As Determined by Different Spectral Methods

proteins	circular dichroism (222 nm)	second-derivative UV (294–291 nm)	fluorescence (335 nm)
bGH	3.8	3.5	3.3[a,b]
8H-hGH	3.6	3.4	3.2[b]
hGH[c]	4.6	4.6	4.6

[a] This result was obtained from Havel et al. (1990). [b] These denaturation midpoints were determined graphically since the fluorescence enhancement that is observed at intermediate GdmCl and low protein concentrations (0.05 mg/mL) precluded standard analysis. [c] Results for hGH were obtained from Brems et al. (1990).

These properties suggest that the corresponding protein region is directly involved in bGH aggregation. The inability of hGH to aggregate through the same mechanism as bGH may be due to differences in their primary structures within this protein region. We have therefore constructed a hybrid bovine/human growth hormone that contains the bovine sequence between residues 1–108 and 134–191 and the human sequence between residues 109 and 133 (8H-bGH) and have compared the folding characteristics of this protein relative to bGH and hGH. We report that although the folding characteristics of the hybrid protein are very similar to bGH, it aggregates to a significantly lesser extent. Therefore, it appears that the formation of the bGH folding intermediate and its subsequent aggregation are dissociable properties.

Materials and Methods

Synthesis of 8H-bGH. Recombinant bovine growth hormone (bGH) was derived from *Escherichia coli* with a temperature-sensitive, runaway plasmid containing the appropriate gene sequence. Gene transcription was performed as previously described (Tomich et al., 1989). Mutagenesis of bGH was performed by replacing the *Pst*I–*Ava*I region coding for amino acid residues 90–132 with oligonucleotides. Plasmid pDH-m4, which contains the bGH-m4 sequence (obtained from Dr. John Mott, The Upjohn Co.) with no *Pst*I site in the vector portion was used for mutagenesis. Plasmid pDH-m4 was treated with *Pst*I and *Ava*I, and the large fragment was isolated and used in the ligation of four oligonucleotides. These four oligonucleotides, assembled as previously described, contain the ends of *Pst*I and *Ava*I and the codons for bGH residues 90–132 with the sibstitutions as shown in Table I. In addition, the oligonucleotides contain a change at codon 105 (without changing the amino acid residue) to generate an Asp^{718} site. The plasmid with the eight mutations is named pDH-m4-8H. The region with the mutations in pDH-m4-8H was sequenced to confirm the changes. For high-level expression of the bGH with these changes, the bGH sequence was cloned into the runaway vector pURA-m4 to give pURA-m4-8H under the control of the *E. coli* tryptophan promoter. Fermentation and isolation of the protein was performed as previously described (Evans & Knuth, 1987). The structure of 8H-bGH was confirmed by tryptic mapping (Hartman et al., 1986) and sequence analysis of isolated tryptic peptides. Pituitary-derived human growth hormone was purchased from Dr. Alan Parlow (UCLA, Harbor Medical Center) and used without further purification.

Peptide Fragments. hGH(96–134) was synthesized on an Applied Biosystems 430A peptide synthesizer (Foster City, CA). Protecting groups were removed, and the resin linkage was cleaved by use of anhydrous HF, and the peptide was purified on reversed-phase HPLC. Yield of the purified peptide was 95 mg (15%). AAA: Asx 6.1 (6), Thr 1.1 (1), Ser 3.9 (4), Glx 4.3 (4), Gly 4.2 (4), Ala 2.0 (2), Val 3.0 (3), Met 1.1 (1), Ile 1.1 (1), Leu 6.2 (6), Tyr 1.9 (2), Phe 0.9 (1), Lys 1.2 (1), Arg 2.1 (2), Pro 1.1 (1). Cs^+ SIMS: m/z 4359.

bGH(96–133) and 8H-bGH(96–133) were isolated following mild trypsin digestion of bGH and 8H-bGH, respectively. The proteins (0.4 mg/mL) were dissolved in 0.1 M ammonium bicarbonate, pH 7.7, and incubated with trypsin (1:500 w/w) at room temperature for 1 h. The digestion was stopped by the addition of GdmCl and purified by reversed-phase HPLC (Vydac C18; The Separations Group, Hesperia, CA). N-Terminal sequence analysis was used to verify the structure of these peptides.

Spectrophotometric Measurements. The amount of secondary structure present in the native proteins was determined by use of a Jasco J-500C circular dichroism spectrophotometer. A 0.1-cm-path-length cell was used; signal intensity was monitored at 222 nm. In addition, aggregation of the partially denatured proteins was monitored at 300 nm in the near-UV CD as previously described (Havel et al., 1986). A 2.0-cm-path-length cell was used in the latter studies. Mean residue ellipticities at 222 and 300 nm ($[\theta]$; deg·cm^2·dmol^{-1}) were calculated by use of the equation

$$[\theta] = (100\theta)/(lcn)$$

where θ is the ellipticity (millidegrees), l is the path length of the cell in centimeters, n is the number of amino acid residues, and c is the millimolar concentration of the protein.

The equilibrium unfolding of these proteins was studied at variable concentrations of GdmCl. Protein unfolding was monitored by far-UV CD, second-derivative UV absorbance, and fluorescence spectroscopy. Second-derivative UV absorbance spectra were obtained by use of an AVIV 14DS UV–vis spectrophotometer and a 5-cm-path-length cell. Fluorescence spectra were obtained by use of an SLM 8000C spectrofluorometer in the photon-counting mode and 1 cm × 4 mm cells. In these experiments, tryptophan was selectively excited at wavelengths of 295 or 300 nm and fluorescence emission was monitored at 335 nm. Equilibrium constants and the free energy of unfolding were calculated from these data by use of the linear extrapolation method (Pace, 1986). Kinetic refolding was monitored by UV absorbance. All experiments were performed at ambient temperature except for the kinetic folding experiments, where noted, and solubility studies, which were performed at 3 °C. Protein concentrations were determined by use of the BCA colorimetric method (Smith et al., 1985).

Equilibrium constants for the aggregation of folding intermediates were determined from near-UV circular dichroism studies in which the 300-nm signal intensity of the partially denatured proteins was monitored as a function of protein concentration. A decrease in MRE parallels the formation of protein aggregate (Havel et al., 1986). In these calculations, a monomer-to-dimer equilibrium was assumed as follows: $2M \leftrightarrow D$, $K_a = [D]/[M]^2$, and total protein = $2[D] + [M]$, where [D] is the concentration of dimer, [M] is the concentration of monomer, and K_a is the association constant. The best fit of the calculated curves to the data was obtained by use of nonlinear least-squares procedures available in ASYST (MacMillan Software).

Precipitation of Aggregated Protein. Quantitative precipitation of aggregated folding intermediates was carried out as previously described (Brems, 1988). In this procedure, aggregation of the folding intermediate was induced by dissolving each protein (2 mg/mL) in 3.7 M GdmCl. After incubation of the protein for 30–60 min at room temperature, aggregated protein was precipitated by dilution of the samples to concentrations of 0.8 M GdmCl and 0.18 mg/mL protein.

Following incubation of the samples for 30 min at room temperature, the amount of precipitation was determined by measuring light scatter at 450 nm with use of an IBM 9420 spectrophotometer.

Analysis of the Kinetic Refolding Data. The kinetic refolding data were analyzed by an On-Line Instrument Systems 3920Z data acquisition and instrument controller (OLIS, Jefferson, GA). The data were fit to a single-exponential kinetic equation by use of fitting routine supplied by OLIS. The kinetic results are presented as time constants of inverse rate.

Size-Exclusion Chromatography. Size-exclusion chromatography was performed by injecting each protein (100 μg/injection) onto a TSK 125 Bio-Sil column (300 × 75 mm; Bio-Rad, Richmond, CA). The protein concentrations used in these studies were 25-fold higher than those used in the spectral studies. This excess was used to compensate for sample dilution that occurs during column elution. The column was eluted with a buffer containing 100 mM Tris·HCl, pH 7.3, and varying amounts of GdmCl as indicated.

Dynamic Light Scattering. Dynamic light-scattering experiments were carried out by the use of a 256-channel autocorrelator (BI-2030; Brookhaven Instruments, Holtsville, NY). A goniometer (BI-2005M, Brookhaven Instruments) was used to define the 90° scattering geometry used in all experiments. An argon ion laser (Lexel 95-4; Cooper Laser Sonics, Palo Alto, CA) operating at 514.5 nm was used as the scattering source. An incident intensity of 50 mW was employed. Samples were checked for photodegradation by measuring UV absorption spectra before and after the scattering experiment. Diffusion coefficients were extracted from the autocorrelation functions by use of the regularization program CONTIN (Provencher 1982a,b). Hydrodynamic radii were then calculated by applying the Stokes–Einstein relationship

$$r = k_B T / 6\pi\eta D_z$$

where r is the Stokes radius (in centrimeters), k_B is the Boltzmann constant, η is the absolute viscosity of the solvent (in centipoises), and D_z is the z-averaged translational diffusion coefficient (in centimeters^2 per second), both determined at the measurement temperature, T, of 25 °C. Sample refractive indexes, kinematic viscosities, and specific gravities were measured with use of commonly available laboratory equipment. Denaturant solutions were clarified by ultrafiltration with a filter having a 500 molecular weight cutoff (XYC05; Amicon, Danvers, MA). Protein samples were dissolved in the denaturant and slowly passed through a 0.2-μm low-protein binding filter (No. 4418; Gelman Science, Ann Arbor, MI) and then through a 0.1-μm polycarbonate membrane filter (110405; Nucleopore, Pleasanton, CA) directly into the scattering cell. The calculated Stokes' radius determined for hGH, dissolved in 6 M GdmCl, was highly variable (±27%). The UV absorption spectra of this solution following laser irradiation did not indicate that degradation had occurred in this sample.

Results

Equilibrium Unfolding Studies of bGH, 8H-bGH, and hGH at Low Concentrations. Equilibrium unfolding studies were undertaken to compare the folding characteristics of bGH, 8H-bGH, and hGH with use of conditions that ensure that these proteins are monomeric (Brems et al., 1985; Havel et al., 1986). Protein concentration was 0.04 mg/mL and the GdmCl concentration was varied from 0 to 6 M. The secondary structural content of the partially denatured proteins was monitored by use of far-UV CD, and the residual tertiary structure was determined by using second-derivative UV absorbance and fluorescence emission spectra. The spectral data were analyzed by use of the linear extrapolation method (Pace, 1986). The denaturation midpoint of bGH, as determined from the far-UV CD signal intensity at 222 nm, was observed at 3.8 ± 0.1 M GdmCl, in agreement with previously reported results (Table I; Brems et al., 1985; Havel et al., 1986). Similarly, the denaturation midpoint of 8H-bGH, as determined by these methods, was observed at 3.6 ± 0.1 M GdmCl. The denaturation midpoints of these proteins, as determined by fluorescence emission and second-derivative UV spectra are also shown in Table I. The data indicate that the secondary structures of bGH and 8H-bGH are more stable then their tertiary structure, indicating that one or more stable intermediates form during protein folding. There were no significant differences in the folding behavior of bGH and 8H-bGH in these experiments. hGH, however, is more resistant to chemical denaturation and unfolds cooperatively.

The fluorescence intensity of the monomeric bGH folding intermediate is enhanced relative to the native protein (Havel et al., 1988). That is, at protein concentrations of 0.05 mg/mL, the fluorescence emission of the partially denatured protein at 350 nm is 30% greater than the denatured protein. Increasing the bGH concentration suppressed this enhancement in fluorescence. No further decreases were observed in signal enhancement above protein concentrations of 0.8 mg/mL. Similarly, the fluorescence intensity of partially denatured, monomeric 8H-bGH (0.04 mg/mL) is enhanced by 25–30% relative to the denatured protein (Figure 2). This finding further indicates that the structures of the bGH and 8H-bGH monomeric folding intermediates are similar.

Far-UV CD spectra of native bGH and 8H-bGH show that both proteins contain about 50% α-helix, and their second-derivative absorption spectra between 250 and 350 nm are virtually superimposable (data not shown). In addition, the far-UV CD and the second-derivative UV absorption spectra of partially denatured bGH and 8H-bGH are similar. These parallels in conformational and unfolding characteristics indicate that these proteins have closely related folding mechanisms.

Aggregation of the Partially Denatured Proteins. In contrast with the similarities noted above, marked differences are observed at elevated protein concentrations with respect to aggregation. The relative propensities of the partially denatured proteins for aggregation have been determined by comparing their relative near-UV CD spectra, solubility, and kinetic refolding rates. For example, a characteristic spectral band at 300 nm in the near-UV CD forms as the result of aggregation of partially denatured bGH (Havel et al., 1986). Although 8H-bGH forms this same spectral band following partial denaturation, the signal intensity is 3-fold lower than is observed for the wild-type protein (Figure 3A). hGH, on the other hand, displays a spectral band of positive ellipticity at 300 nm below 4 M GdmCl, and this spectral band decreases cooperatively as the protein unfolds.

The concentration dependence of the 300-nm signal was used to determine the association constant of protein aggregation (Figure 3B). At all concentrations greater than 0.04 mg/mL, the spectral intensity observed for bGH exceeded that of 8H-bGH. For example, at 9 mg/mL, the negative 300-nm signal for partially denatured bGH is 2-fold greater than that observed for 8H-bGH. Equilibrium constants for aggregation were calculated from these data. Assuming that aggregates of these proteins consist primarily of dimers, calculation of

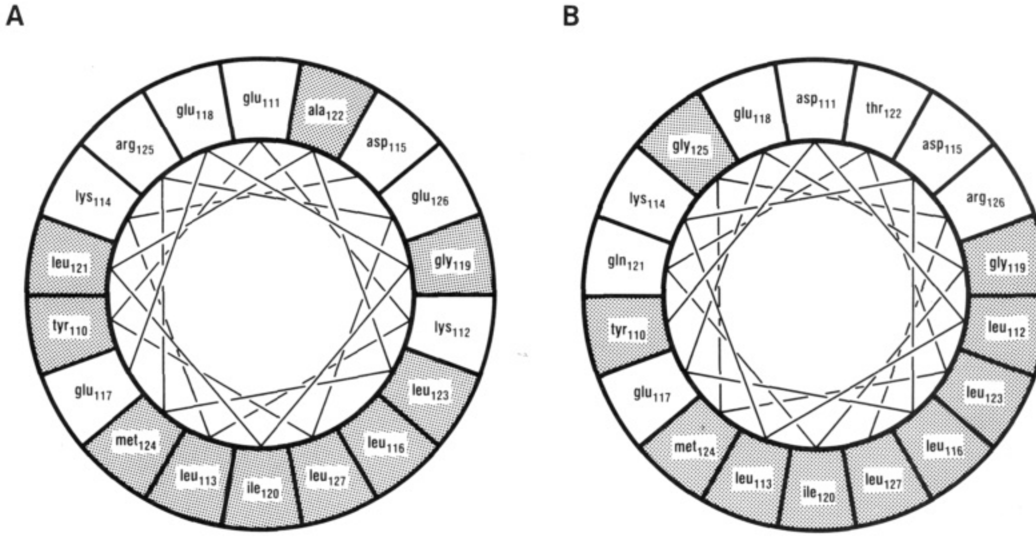

C

```
                                    100
bGH     : H-VAL-PHE-THR-ASN-SER-LEU-VAL-PHE-GLY-THR-SER-ASP-   -
8H-bGH  :
hGH     :           ALA                 TYR     ALA         SER

                      110                                  120
bGH     :  ARG-VAL-TYR-GLU-LYS-LEU-LYS-ASP-LEU-GLU-GLU-GLY-ILE-
8H-bGH  :  ASN             ASP LEU
hGH     :  ASN             ASP LEU

                                                 130
bGH     :  LEU-ALA-LEU-MET-ARG-GLU-LEU-GLU-ASP-GLY-THR-PRO-ARG-OH
8H-bGH  :  GLN THR         GLY ARG             SER
hGH     :  GLN THR         GLY ARG             SER
```

FIGURE 1: Helical wheel analyses of (A) residues 110–127 of bGH and (B) 110–127 of hGH. The hGH primary sequence in this region is identical with residues 110–127 of 8H-bGH. Hydrophobic amino acids, noted by the shading, are designated as described by Eisenberg et al. (1984). Panel C shows parimary sequence comparisons of bGH, 8H-bGH, and hGH between residues 96 and 133.

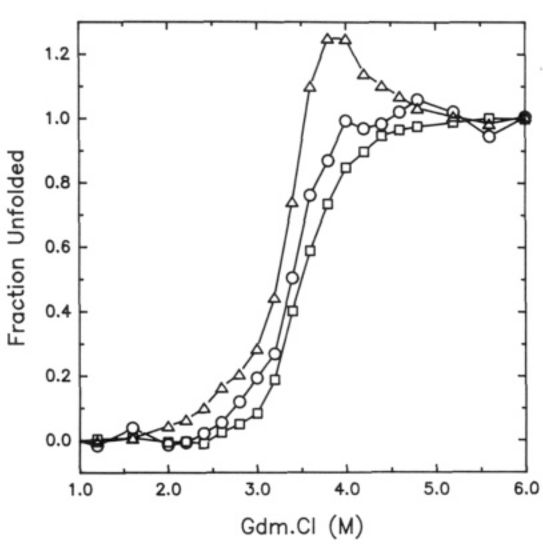

FIGURE 2: Equilibrium denaturation of 8H-bGH. This protein was dissolved in a buffer containing 50 mM NH_4HCO_3 (pH 8.5) and variable concentrations of GdmCl. Denaturation was monitored by use of the following three probes: circular dichroism at 222 nm (□), tryptophan fluorescence (△), and second-derivative UV absorbance difference spectra at 291 and 294 nm (○). The concentration of 8H-bGH in these experiments was 0.04 mg/mL. The fraction of unfolded protein is expressed as follows: fraction unfolded = $(x_{\text{folded}} - x_{\text{sample}})/(x_{\text{folded}} - x_{\text{unfolded}})$.

the bGH monomer and dimer MRE values at 300 nm are 1 and −128 ± 5 deg·cm^2·dmol^{-1}, respectively. Similarly, the MRE values of the 8H-bGH monomer and dimer are −4 and −82 ± 5 deg·cm^2·dmol^{-1}, respectively. Using these estimates, nonlinear least-squares analyses suggest that equilibrium constants for the aggregation of bGH and 8H-bGH differ by 1 order of magnitude (1.6×10^5 and 1.4×10^4 M^{-1}, respectively). The positive ellipticity in the near-UV CD previously noted for hGH is independent of protein concentration (Figure 3B).

Solubility in the Two-Step Precipitation Assay. A two-step precipitation assay has been shown to correlate with the amount of aggregated protein that forms on partial denaturation (Brems, 1988). This assay is based on the relative insolubility of the partially unfolded aggregate relative to the native and unfolded states. In this assay, we found that 70, 34, and 0% of the added bGH, 8H-bGH, and hGH precipitates, respectively (Figure 4A).

Kinetic Refolding Studies. The refolding kinetics of bGH have been previously shown to be described by two first-order reactions. These reactions include a fast, concentration-independent phase and a slower, concentration-dependent phase (Brems et al., 1987a). The slower phase is due to refolding from the aggregated state. Consistent with this finding, a bGH analogue that contains leucine at position 112, a structural change that stabilizes the aggregated folding intermediate, refolds more slowly than wild-type bGH at equivalent concentrations (Brems et al., 1988). As expected, the fast refolding phase of the Leu^{112} analogue was not affected by this structural change. Kinetic refolding studies of 8H-bGH show that the slow, concentration-dependent folding phase occurs more quickly than is observed for bGH (Figure 5). At rel-

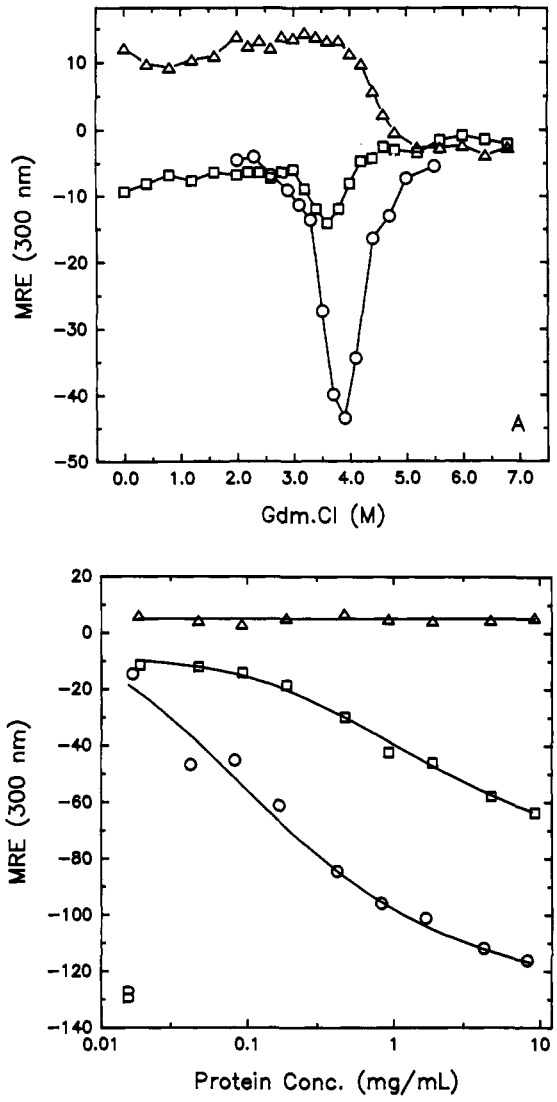

FIGURE 3: Near-UV CD at 300 nm for bGH (○), 8H-bGH (□), and hGH (△) as a function of GdmCl and protein concentration. (A) Each protein (0.13 mg/mL) was dissolved in 50 mM ammonium bicarbonate (pH 8.5), containing variable concentrations of GdmCl. Measurements were obtained at ambient temperature. (B) Solutions contained variable concentrations of each protein dissolved in 50 mM ammonium bicarbonate (pH 8.5) containing 3.7 M GdmCl for bGH and 8H-bGH and 4.6 M GdmCl for hGH. Solid lines for bGH and 8H-bGH represent calculated curves assuming a monomer–dimer model. The best fit of the calculated curves to the data was obtained by use of nonlinear least-squares procedures available in ASYST (MacMillan Software).

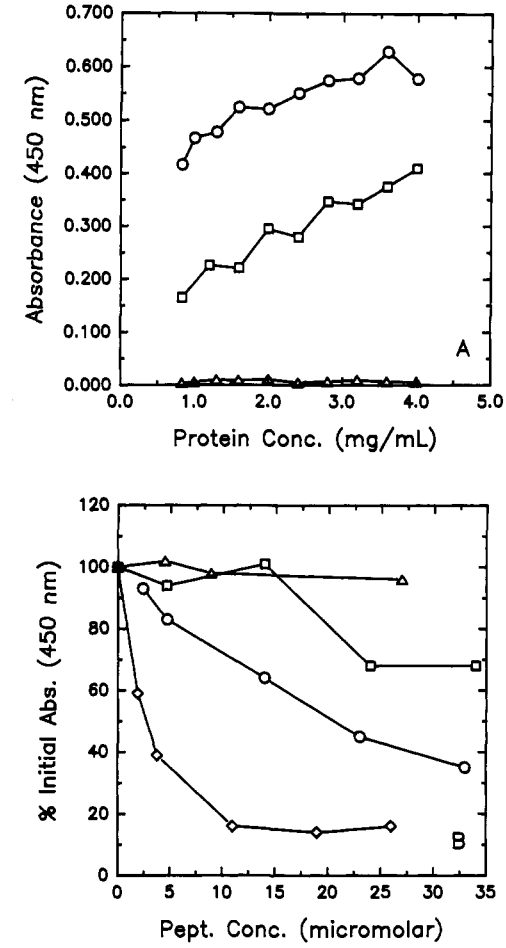

FIGURE 4: Determination of the extent of protein aggregation using the two-step precipitation assay. (A) Solubility of bGH, 8H-GH, and hGH is shown as a function of protein concentration. The two-step procedure has been described previously (Brems, 1988). Key: bGH (○), 8H-bGH (□), and hGH (△). Protein concentrations were determined by use of the BCA method (Smith et al., 1985). (B) The effect of bGH(95–133), 8H-bGH(96–133), hGH(96–134), and [Leu^{112}]bGH(96–133) on the precipitation of aggregated bGH is shown. Variable concentrations of each peptide were added during the first step of the two-step procedure. For these experiments, temperature was maintained at 3.2 °C. The final bGH concentration in these experiments was 8 μM. Readings were taken 15 min after dilution. Key: bGH (○), 8H-bGH (□), hGH (△); [Leu^{112}]bGH (◇).

atively low concentrations (<0.4 mg/mL), the relaxation times for the slow refolding phase of bGH and 8H-bGH are 122 and 131 s, respectively. At higher protein concentrations (4 mg/mL), the relaxation time for the slow refolding phase of 8H-bGH is 1.5 times faster than the corresponding refolding phase of bGH, 175 vs 270 seconds, respectively. hGH refolds significantly faster than bGH or 8H-bGH and is independent of protein concentration between 0.1 and 4 mg/mL.

Size-Exclusion Chromatography. Size-exclusion chromatography of these proteins, as a function of GdmCl concentration, also suggests that bGH and 8H-bGH aggregate to differing extents (Figure 6). In order to compensate for on-column dilution, the injected protein concentrations were 1 mg/mL, 25-fold more concentrated than the protein concentrations used in the fluorescence experiments discussed above. The retention times of hGH on the SEC column shifts to shorter retention times as the protein unfolds, and the midpoint of this change coincides with the denaturation midpoint of this protein (4.6 M GdmCl; Brems et al., 1990). In contrast, the midpoint of this shift in size-exclusion retention times of bGH and 8H-bGH is observed at 3.3 M GdmCl, which is about 0.4 M lower than the denaturation midpoints of these proteins as determined by far-UV CD. This finding suggests that significant aggregation of these proteins occurs before they lose 50% of their secondary structure. Maximum aggregation for bGH occurs between 3.7 and 4 M GdmCl, and this species elutes 0.4 min earlier than the corresponding 8H-bGH species. The variability of retention times in the chromatography system was ± 0.1 minute. This experiment confirms that wild-type protein aggregates to a greater extent than the bGH analogue.

Dynamic Light Scattering. Dynamic light-scattering studies of bGH, 8H-bGH, and hGH show that in nondenaturing media (≤2 M GdmCl) the radius of each protein is 1.8 ± 0.2 nm (Table II). Partial denaturation of these proteins (3.7 M GdmCl; 0.5 mg/mL) increases the radii of bGH, 8H-bGH, and hGH to 4.3 3.7, and 2.2, all ± 10%, respectively. Increasing the concentration of GdmCl to 6 M decreases the

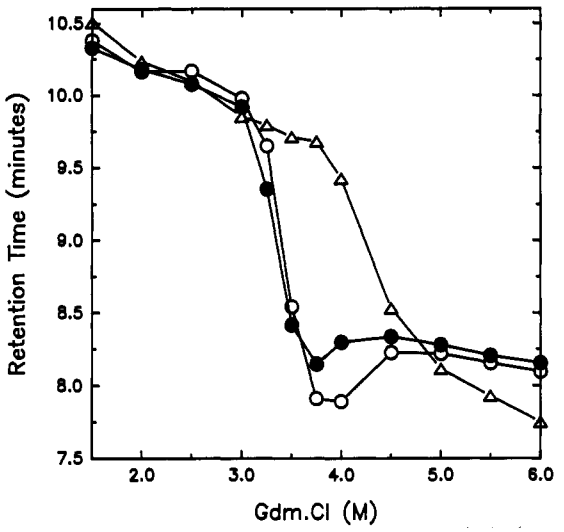

FIGURE 5: Slow-phase folding rates of bGH, 8H-bGH, and hGH as a function of protein concentration. Each protein was dissolved in 50 mM ammonium bicarbonate, pH 8.5/6 M GdmCl and maintained at 3 °C. A 10-fold dilution of these samples yielded final solutions containing 2.2 M GdmCl and variable protein concentrations. Key: bGH (○); 8H-bGH (□); hGH (△).

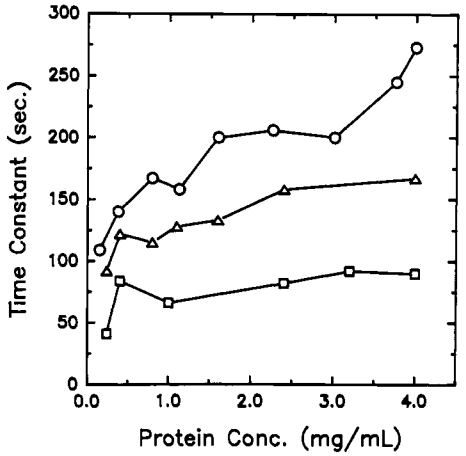

FIGURE 6: Size-exclusion HPLC of bGH, 8H-bGH, and hGH as a function of GdmCl and protein concentration. bGH (○), 8H-bGH (●), and hGH (△) (1 mg/mL) were preequilibrated in the eluting buffer, which contained 1.5–6 M GdmCl as noted. A total of 100 μL of each solution was injected. Chromatography conditions: TSK 125 (Bio-Sil, 300 × 7.5 mm; Bio-Rad, Richmond, CA), flow rate 1 mL/min. UV absorption was monitored at 214 nm.

Table II: The Hydrodynamic Radii of Native, Partially, Denatured, and Fully Denatured Growth Hormones

	GdmCl (M)		
proteins	2.0	3.7	6.0
bGH	1.9[a]	4.3	2.1
hGH	1.7	2.2	2.2
8H-bGH	1.8	3.7	2.1

[a] Numbers represent the Stokes radii determined from the light-scattering data (in nanometers). Estimated precision is ± 10%.

hydrodynamic radii of bGH and 8H-bGH to about 2.1 nm. The lower hydrodynamic radii of the fully denatured proteins, relative to the partially denatured proteins, indicate that the hydrodynamic radii determined at intermediate GdmCl concentrations are not artifacts due to the presence of chaotrope. These data suggest that the partial denaturation of bGH at elevated protein concentration, and to a lesser extent, 8H-bGH, leads to aggregation. hGH does not appear to aggregate in these experiments.

The differences in the hydrodynamic radii of each native and fully denatured protein differ only by 10–20%. This is similar to changes observed in the hydrodynamic radii of lysozyme, ribonuclease, and chymotrypsinogen following denaturation. The hydrodynamic radii of these proteins increase by 18, 18, and 26%, respectively (Nicoli & Benedek, 1976). The polydispersity of solutions containing aggregated partially denatured protein precluded the quantitation of the aggregated species and the determination of equilibrium association constants from dynamic light-scattering studies.

The Effects of bGH(96–133) and Analogues on the Aggregation of bGH. Coincubation of bGH with bGH(96–133) in the first step of the two-step solubility assay has been shown to decrease the aggregation of partially denatured bGH (Brems, 1988). We obtained the corresponding peptides from 8H-bGH and hGH as described above and compared the abilities of these peptides to inhibit the precipitation of aggregated bGH. At a peptide concentration of 32 μM, the molar ratio of peptide:protein was 4:1. At this relative concentration, bGH(96–133), 8H-bGH(96–133) and hGH(96–134) inhibit bGH precipitation by 68, 36, and 0%, respectively (Figure 4B). The ability of these compounds to inhibit bGH precipitation decreased at lower peptide concentrations. Therefore, the ability of these fragments to inhibit bGH aggregation parallels the relative aggregation of the parent proteins. [Leu^{112}]bGH(96–133), obtained previously, was more effective at inhibiting bGH precipitation in this assay than any of the other peptides tested (Lehrman et al., 1990). This is consistent with the enhanced stability of the [Leu^{112}]bGH aggregate (Brems et al., 1988). These findings suggest that the diminished aggregation of 8H-bGH is due primarily to local structural changes between residues 96 and 133 rather than effects on overall protein conformation.

Discussion

Previous studies have demonstrated that bGH folds via the pathway shown below (Brems, 1988)

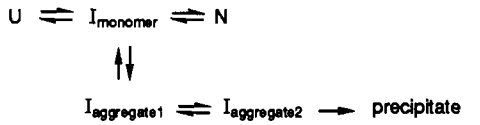

where U, I, and N represent unfolded, intermediate folded, and native proteins, respectively. This scheme illustrates that the folding of bGH is a multistate process involving at least one folding intermediate and that formation of the monomeric intermediate precedes aggregation. The scheme implies that changes in bGH primary structure can dissociate the folding and aggregation processes. The data presented here confirm this prediction. Although no significant differences were observed in the folding behavior of bGH and 8H-bGH, partially denatured bGH aggregates to a significantly greater extent than partially denatured 8H-bGH. The data supporting this conclusion are summarized as follows. The equilibrium unfolding behaviors of bGH and 8H-bGH were not significantly different when monitored by spectral probes that are sensitive to secondary and tertiary structure. The fluorescence intensity of bGH and 8H-bGH increased by 25–30% at low protein (<10 μM) and intermediate concentrations of GdmCl, respectively. In addition, spectral properties of native and partially denatured forms of both proteins were not significantly different. On the other hand, partially denatured bGH aggregates more than partially denatured 8H-bGH at high protein and intermediate GdmCl concentrations. For example, the 300-nm CD band of partially denatured bGH is greater in amplitude than that of the partially denatured 8H-bGH at

all protein concentrations tested. Similarly, bGH precipitates more than 8H-bGH in the two-step assay and refolds at a rate slower than that of 8H-bGH at all protein concentrations tested. The equilibrium constant for bGH aggregation, as determined from the near-UV CD data, is 10-fold greater than that calculated for 8H-bGH aggregation. Data from dynamic light-scattering experiments and size-exclusion chromatography also suggest that bGH aggregates to a greater extent than 8H-bGH.

Differences between the primary structures of wild-type bGH and 8H-bGH are limited to the third α-helix of the four-α-helix bundle. The altered residues may directly participate in interactions that stabilize the protein aggregate, or they may indirectly affect aggregation by altering protein conformation. Although these studies do not discount the possibility that one or more of these residues participate in intermolecular contacts that stabilize the protein aggregate, we suggest that these modifications decrease the amount of aggregation observed in 8H-bGH by diminishing α-helicity in this region of the protein. This suggestion is supported by the prediction that these modifications reduce α-helicity in this protein region by about one turn near the C-terminal end (Robson & Pain, 1971). Far-UV CD studies of bGH(96–133) and hGH(96–134) indicate that the latter fragment, which has the same primary structure as 8H-bGH within the α-helical region, has significantly less α-helical potential than the corresponding bGH fragment (Lehrman et al., 1990). Recent experiments confirm that the corresponding 8H-bGH peptide closely resembles hGH(96–134) in its propensity for α-helix formation (S.R.L. and M. E. Lund, unpublished data). Long-range conformational changes are less likely to account for the observed behavior since (1) the α-helical content of bGH and 8H-bGH is approximately equal and (2) the behavior of bGH(96–133) and 8H-bGH(96–133) parallels that of their parent proteins in the two-step precipitation assay.

Not all eight amino acid subtitutions destabilize the aggregation of partially denatured protein. At least one of the amino acid substitutions in 8H-bGH, the substitution of leucine at position 112, stabilizes the formation of the protein aggregate (Brems et al., 1988). This finding is reasonable since the isobutyl side chain of leucine enhances the hydrophobic effect without diminishing the α-helical potential of this protein region. Therefore, some or all of the seven remaining substitutions in 8H-bGH compensate for this stabilizing effect of Leu^{112} on protein aggregation. Since these eight amino acid substitutions do not totally eliminate aggregation, other bGH regions must also help stabilize this species.

Recent studies on the refolding and aggregation behavior of hGH show that the reduction and acylation of cysteine residues in hGH, modifications that decrease the conformational stability of that protein, result in the formation of folding intermediates that undergo aggregation (Brems et al., 1990). It was concluded from this study that the structural features responsible for the formation of folding intermediates in bGH are also present in hGH but that the relative stability of native hGH precludes the observation of folding intermediates. Therefore, aggregation can be minimized by (1) directly eliminating interactions that stabilize aggregation or (2) precluding the formation of folding intermediates. Note that since the destabilized form of hGH can aggregate via folding intermediates, modifications of other bGH regions to conform with the hGH sequence cannot always be expected to diminish aggregation.

The generality of these findings could be established by studying the folding behavior of other proteins that contain amphipathic regions and that refold via two-state mechanisms. We predict that these proteins will aggregate if structural modifications permit the formation of stable folding intermediates that expose these amphipathic structures. In addition, previous studies of proteins that refold via multistate mechanisms support the generality of the behavior described above. These studies suggest that aggregation of partially denatured bGH may result from interactions that resemble those of the native conformation. For example, tryptophanase aggregates at elevated concentrations following partial denaturation (London et al., 1974). The intermolecular interactions that stabilize the aggregate appear to be similar to those of the native enzyme. Similarly, refolding studies of rhodanese suggest that this enzyme forms an aggregate that is stabilized by intermolecular hydrophobic effects between regions that retain native-like secondary structure (Horowitz & Criscimagna, 1990). Therefore, aggregation of partially denatured bGH may result from intermolecular pairing of the α-helix that spans residues 108–127 (α-helix 3), with α-helices that span residues 7–34 (α-helix 1) and 75–96 (α-helix 2; Abdel-Meguid et al., 1987). Note that in growth hormone the elongated protein strands connecting α-helices 1 and 2, and 3 and 4, permit separation of these α-helical pairs without concomitant loss of protein secondary structure (Abdel-Meguid et al., 1987). This intramolecular unpairing of α-helices would permit intermolecular pairing as suggested above and would be stabilized via the hydrophobic effect. Other α-helical bundle proteins such as cytochrome b_{562} and hemerythrin have different connectivity between adjacent α-helices and are not expected to aggregate by this mechanism.

Acknowledgments

We gratefully acknowledge the efforts of Drs. J. Mott, R. Kirschner, A. Parcells, and J. Hoogerheide and M. Sears, P. Davidson, L. Snyder, N. Haner, C. Campbell, and K. Schlukebir in the synthesis of 8H-bGH. We also thank Paul Elzinga for calculating the equilibrium constants from the near-UV–CD data, Drs. F. Kezdy, and T. J. Thamann for their critical comments on the manuscript, and Sharon Andrews for her secretarial assistance.

Registry No. bGH, 9002-72-6.

References

Abdel-Meguid, S. S., Shieh, H.-S., Smith, W. W., Dayringer, H. E., Violand, B. N., & Bentle, L. A. (1987) *Proc. Natl. Acad. Sci. U.S.A. 84*, 6434–6437.

Brems, D. N. (1988) *Biochemistry 27*, 4541–4546.

Brems, D. N., & Havel, H. A. (1989) *Proteins: Struct., Funct., Genet. 5*, 93–95.

Brems, D. N., Plaisted, S. M., Harvel, H. A., Kauffman, E. W., Stodola, J. D., Eaton, L. C., & White, R. D. (1985) *Biochemistry 24*, 7662–7668.

Brems, D. N., Plaisted, S. M., Kauffman, E. W., & Havel, H. A. (1986) *Biochemistry 25*, 6539–6543.

Brems, D. N., Plaisted, S. M., Dougherty, J. J., & Holzman, T. F. (1987a) *J. Biol. Chem. 262*, 2590–2596.

Brems, D. N., Plaisted, S. M., Kauffman, E. W., Lund, M. E., & Lehrman, S. R. (1987b) *Biochemistry 26*, 7774–7778.

Brems, D. N., Plaisted, S. M., Havel, H. A., & Tomich, C.-S. C. (1988) *Proc. Natl. Acad. Sci. U.S.A. 85*, 3367–3371.

Brems, D. N., Brown, P. L., & Becker, G. W. (1990) *J. Biol. Chem. 265*, 5504–5511.

Burger, H. G., Edelhoch, H., & Condliffe, P. G. (1966) *J. Biol. Chem. 260*, 8520–8525.

Chou, P. Y., & Fasman, G. (1978) *Annu. Rev. Biochem. 47*, 251.

Eisenberg, D., Weiss, R. M., & Terwilliger, T. C. (1984) *Proc. Natl. Acad. Sci. U.S.A. 81*, 140.
Evans, T. W., & Knuth, M. W. (1987) World Patent WO 8700204, January 15, 1987.
Hartman, P. A., Stodola, J. D., Harbour, G. C., & Hoogerheide, J. G. (1986) *J. Chromatogr. 360*, 385-395.
Havel, H. A., Kauffman, E. W., Plaisted, S. M., & Brems, D. N., (1986) *Biochemistry 25*, 6533-6538.
Havel, H. A., Kauffman, E. W., & Elzinga, P. A. (1988) *Biochim. Biophys. Acta 955*, 154-163.
Holladay, L. A., Hammonds, R. G., & Puett, D. (1974) *Biochemistry 13*, 1653-1661.
Horowitz, P. M., & Criscimagna, N. L. (1990) *J. Biol. Chem. 265*, 2576-2583.
Lehrman, S. R., Tuls, J. L., & Lund, M. E. (1990) in *Peptides: Proceedings of the Eleventh Peptide Symposium* (Rivier, J. E., & Marshall, G. R., Eds.) pp 571-574, ESCOM Publishers, Leiden, The Netherlands.
London, J. Skrzynia, C., & Goldberg, M. E. (1974) *Eur. J. Biochem. 47*, 409.
Nicoli & Benedek (1976) *Biopolymers 15*, 2421-2437.
Pace, C. N. (1986) *Methods Enzymol. 131*, 266.
Provencher, S. W. (1982) *Comput. Phys. Commun. 27*, 213-227, 229-242.
Robson, B., & Pain, R. H. (1971) *J. Mol. Biol. 58*, 237.
Smith, P. K., Krohn, R. I., Hermanson, G. T., Mallia, A. K., Gartner, F. H., Provenzano, M. D., Fujimoto, E. K., Goeke, N. M., Olson, B. J., & Klenk, D. C. (1985) *Anal. Biochem. 150*, 76-85.
Stolar, M. W., Amburn, K., & Baumann, G. (1984) *J. Clin. Endocrinol. Metab. 59*, 212.
Tomich, C.-S. C., Olson, E. R., Olsen, M. K., Kaytes, P. S., Rockenbach, S. A., & Hatzenbuhler, N. T. (1989) *Nucleic Acids Res. 17*, 3179-3197.

Characterization of a Synthetic Peptide Corresponding to a Receptor Binding Domain of Mouse Interferon γ[†]

Harold I. Magazine* and Howard M. Johnson
Department of Microbiology and Cell Science, University of Florida, Gainesville, Florida 32611
Received December 12, 1990; Revised Manuscript Received March 1, 1991

ABSTRACT: A receptor binding region of mouse interferon γ (IFNγ) has previously been localized to the N-terminal 39 amino acids of the molecule by use of synthetic peptides and monoclonal antibodies. In this report, a detailed analysis of the synthetic peptide corresponding to this region, IFNγ(1-39), is presented. Circular dichroism (CD) spectroscopy indicated that the peptide has stable secondary structure under aqueous conditions and adopts a combination of α-helical and random structure. A peptide lacking two N-terminal amino acids, IFNγ(3-39), had similar secondary structure and equivalent ability to compete for receptor binding, while peptides lacking four or more N-terminal residues had reduced α-helical structure and did not inhibit ^{125}I-IFNγ binding. Substitution of proline, a helix-destabilizing amino acid, for leucine (residue 8) of a predicted amphipathic α-helix (residues 3-12), IFNγ(1-39)[Pro]^{8}, resulted in a substantial reduction in the helical content of the peptide, supporting the presence of helical structure in this region. However, destabilization of the helix did not reduce the competitive ability of the peptide. A peptide lacking eight C-terminal residues, IFNγ(1-31), did not block ^{125}I-IFNγ binding and had no detectable α-helical structure, suggesting a requirement of the predicted second α-helix (residues 20-34) for receptor interaction and helix stabilization. Substitution of phenylalanine for tyrosine at position 14, IFNγ(1-39)[Phe]^{14}, a central location of a predicted Ω-loop structure, did not affect the secondary structure associated with the region yet resulted in a 30-fold increase in receptor competition. Substitution with glycine at position 14 also did not affect secondary structure and resulted in a competitive ability similar to that of IFNγ(1-39). These data support the presence of a binding domain in the N-terminus of IFNγ and indicate a role for residues 3, 4, 14, and at least some of residues 32-39 in IFNγ(1-39) interaction with receptor. This study provides insight into the structural/functional basis for IFNγ interaction with receptor that should be useful for the development of potent agonists and antagonists of IFNγ action.

Interferon γ (IFNγ)[1] is a secretory glycoprotein produced primarily by antigen- and mitogen-stimulated T-lymphocytes and plays a central role in the initiation and regulation of the immune response (Johnson, 1985). IFNγ regulates class II major histocompatibility complex antigen expression, B-cell maturation, and antibody production as well as the activation of the host defense against tumor cells and microorganisms [reviewed by Vilcek et al. (1985)]. Although the mouse and human IFNγ receptor has been cloned recently (Auget et al., 1988; Gray et al., 1989; Kumar et al., 1989), the mechanism by which IFNγ exerts its many biological activities remains unclear.

[†] This work was supported by Research Grant CA 38587 from the National Institutes of Health. Florida Agricultural Experimental Station, Journal Series No. R-01566.
* To whom all correspondence should be addressed at The Albany Medical College, Department of Biochemistry A-10, 47 New Scotland Ave., Albany, NY 12208.

[1] Abbreviations: IFNγ, interferon γ; CD, circular dichroism; mAb, monoclonal antibody; tBoc, *tert*-butyloxycarbonyl; PAM, (phenylacetamido)methyl; HPLC, high-performance liquid chromatography; FBS, fetal bovine serum; TFE, 2,2,2-trifluoroethanol.

0006-2960/91/0430-5784$02.50/0